Photochemical & Photobiological Sciences

Dynamic Article Links

Cite this: *Photochem. Photobiol. Sci.*, 2012, **11**, 1081

www.rsc.org/pps

PAPER

The mechanism of the photochromic transformation of spirorhodamines†‡

Hugo Montenegro, Matías Di Paolo, Daiana Capdevila, Pedro F. Aramendía and Mariano L. Bossi*

Received 10th December 2011, Accepted 26th March 2012
DOI: 10.1039/c2pp05402g

We investigate the equilibrium, kinetics, and mechanism of the photochromic transformation of a series of amido spirorhodamine compounds—differing in the nature of the substituents of the amido group and in the rhodamine chromophore—in ethanol at room temperature in the presence of trifluoroacetic acid. A proton participates in the equilibrium between the spiro form and the open rhodamine form. The relaxation times in the dark or under continuous irradiation show a linear dependence on the proton concentration. The slopes of these plots show a linear free energy relation with the equilibrium constant of the transformation. A mechanism involving reversible reaction steps between four states: the two thermodynamically stable isomers, a protonated spiro form, and a deprotonated open form, can account for the kinetic observations in the dark and under irradiation.

Introduction

Much work has been devoted to the study of photochromic compounds because of the switching possibility between two distinct molecular states.[1–4] The remote, wireless, light driven control of the composition of the system and the different characteristics of the two isomeric forms of the compound lead to a broad variety of applications such as information storage,[5] alignment of liquid crystals,[6] or photomechanical applications.[7,8]

Recently, photochromic systems have been utilized in fluorescence imaging applications to obtain super-resolution by controlled activation of emitting chromophores.[9–11] This application requires the switching of the probe between two distinct molecular states, in this case the thermodynamically stable isomers of the photochromic system, where at least one of them must be highly fluorescent. This requirement imposes a great restriction, because among the many known photochromic systems,[1,2] only a few have a fluorescent isomer. Spirorhodamines[12] are a family of photochromic compounds that display intrinsic fluorescence. Both the properties of the bright state and the reliable control of the photoswitchable emission meet the requirements for super-resolution imaging.[13] Hence, they have found important applications as molecular probes in imaging techniques based on the switching and localization of single fluorophores.[14] The photochromic transformation of spirorhodamines is illustrated in Scheme 1.

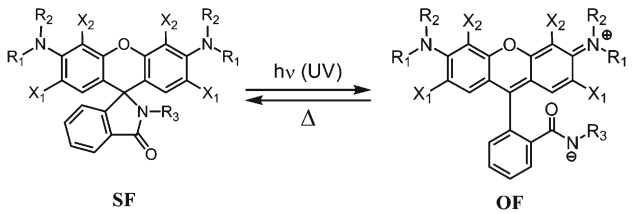

Scheme 1 Photochromic transformation of spirorhodamines.

Depending on the substitution pattern on the chromophore, particularly the substituents in the amino groups (R_1 and R_2 in Scheme 1), the open form absorbs strongly in the blue–green range of the visible spectrum and emits in the green–red portion with an emission quantum yield often greater than 0.5.[15,16] The spiro form only absorbs in the UV range and is non emissive. The transformation of the spiro form to the open form proceeds thermally as well as photochemically, whereas the ring closure is a thermal reaction. Since the first report on the kinetics of some photochromic rhodamines in 1977,[12] only isolated studies on the kinetics and the mechanism of the transformation have been carried out.[17]

In view of the renewed interest in this family of photochromic compounds, triggered by their recent applications in fluorescence nanoscopy,[13,14,18–20] we undertook a kinetic and mechanistic study of the photochemical and thermal ring aperture and the thermal ring closure for a series of model spirorhodamine dyes with differing substituents (Scheme 2) with the aim of understanding the factors controlling the kinetics and the equilibrium of the photochromic transformation.

Materials and methods

Preparation of the photochromic fluorescent probes

(See ESI‡ for details.) Compounds **3–6** were prepared from two commercial rhodamines, rhodamine B (Sigma-Aldrich, dye

INQUIMAE and Departamento de Química Inorgánica, Analítica y Química Física, Facultad de Ciencias Exactas y Naturales, Universidad de Buenos Aires, Pabellón 2, Ciudad Universitaria, 1428 Buenos Aires, Argentina. E-mail: mariano@qi.fcen.uba.ar

† This article is published as part of a themed issue in honour of Professor Kurt Schaffner on the occasion of his 80th birthday.

‡ Electronic supplementary information (ESI) available. See DOI: 10.1039/c2pp05402g

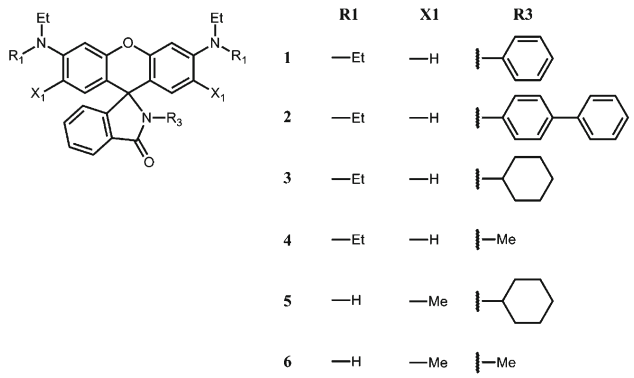

Scheme 2 Structure of the compounds used in this study.

content ~95%, compounds **3**–**4**) and rhodamine 6G (Sigma-Aldrich, dye content ~95%, compounds **5**–**6**) by a known procedure.[21–23] Briefly, 100 mg of rhodamine 6G or rhodamine B ethyl ester were dissolved in 3 mL of dry DMF (Merck, Analytical Grade) and then a 10 fold molar excess of the amine was added. The samples were left to react in the dark under vigorous magnetic stirring at room temperature for 16 h. Then, the reaction mixture was poured into a mixture of crushed ice and water to precipitate the product. The sample was first separated from unreacted products by two centrifugation cycles (redispersed in DMF and precipitated again in cold water), and finally purified by column chromatography to afford white powders (10% yield for compound **3**, 12% yield for compound **4**, 68% yield for compound **5**, and 36% yield for compound **6**). Rhodamine B ethyl ester was prepared by refluxing rhodamine B (500 mg) in ethanol (50 ml) with catalytic amounts of sulfuric acid (*ca.* 0.3 ml) for 4 h. Then, the reaction mixture was neutralized with $NaHCO_3$ (s.s.) and extracted with CH_2Cl_2. After the solvent was evaporated a purple powder was obtained (84% yield) and directly used to prepare compounds **3** and **4**. Compounds **1**–**2** were kindly provided by Dr Vladimir Belov (Department of NanoBiophotonics, Max-Planck-Institut für Biophysikalische Chemie, Göttingen, Germany).

Absorption and fluorescence spectroscopy

Steady state absorption and fluorescence spectra, as well as kinetic measurements with either absorption or fluorescence emission detection, were performed in a Shimadzu UV-Visible spectrophotometer model UV-1603 or in a PTI Quantamaster fluorescence spectrofluorometer. In a typical experiment, a 2.3 μM solution of the photochromic compound was prepared in absolute ethanol (J.T. Baker, Analytical Grade) and the absorption spectrum of the closed isomer was measured. Then, a small amount of a concentrated stock solution of trifluoroacetic acid (TFA, Fluka, purum grade ≥98.0%) in ethanol was added to a desired final concentration in the 10^{-1}–10^{-4} M range and the emission intensity of the open form was recorded as a function of time, to determine the thermal relaxation of the system. Excitation wavelength was 520 nm and emission detection was set to 580 nm for compounds **1**–**4** and 550 nm for compounds **5**–**6**. After equilibrium was reached, the absorption spectrum was recorded again to determine the rate of conversion to the open form and the equilibrium constant. Then, the sample was

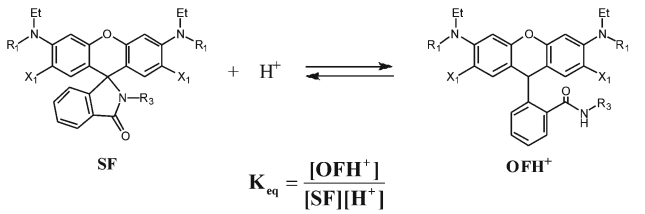

Scheme 3 Equilibrium of the proton assisted spirorhodamine transformation.

irradiated at 315 nm (3.9×10^{-10} E cm^{-2} s^{-1}) in the spectrofluorometer for intervals of 1 to 6 min (depending on the studied compound) and the progress of the photochemical reaction was monitored as a function of irradiation time at the same excitation and emission conditions used for the thermal process (irradiation at 315 nm was interrupted during open form emission monitoring). When the photostationary state was reached, irradiation in the UV was ceased and the thermal relaxation was again recorded under the same conditions.

Results

Dark ring opening and protonation equilibrium

Spirorhodamines form an open ring protonated form which absorbs and emits with similar characteristics as the parent rhodamine dye (OFH^+ in Scheme 3).[20] The coloration of solutions of the spiro form (SF in Scheme 3), and thus the conversion rate to the OFH^+ (open form), depends on the pH of the solution and on the substitution pattern on the chromophore (Fig. 1a). We first studied this dark equilibrium for compounds **1**–**6**, considering that only two species are present, according to Scheme 3.

Considering the fact that the total TFA concentration is much larger than the analytical spirorhodamine concentration, and assuming that TFA is fully dissociated, we expect a linear dependence between the inverse absorbance at the maximum of the OFH^+ form and the inverse of proton concentration, according to eqn (1) (see ESI‡ for the derivation).

$$\frac{1}{A_{\infty}^{VIS}} = \frac{1}{A^{\diamond}} + \frac{1}{K_{eq} \cdot A^{\diamond}} \cdot \frac{1}{[H^+]}; \quad A^{\diamond} = A_0^{UV} \cdot \left(\frac{\varepsilon_{OFH^+}^{VIS}}{\varepsilon_{SF}^{UV}} \right) \qquad (1)$$

where A_0^{UV} is the initial absorption at the maximum of the SF (*ca.* 313 nm), A_{∞}^{VIS} is the final absorbance in the visible, at the maximum of OFH^+, $\varepsilon_{isomer}^{\lambda}$ are the corresponding molar absorption coefficients, $[H^+]$ is set equal to the total TFA concentration under the assumption of complete dissociation. The optical path *l* is, in all cases, 1 cm and thus was omitted.

A plot of the spectral data shown in Fig. 1A, according to eqn (1) is shown in Fig. 1B for compound **5**. In view of the good correlation, we conclude that the proton itself is the actual protonating agent in the equilibrium. In a similar way the equilibrium constant is calculated for each of the other spirorhodamines. All values are summarized in Table 1.

Kinetics of the involved reactions

Three kinetic runs with differing TFA concentration were successively measured for each compound and kinetic characteristic

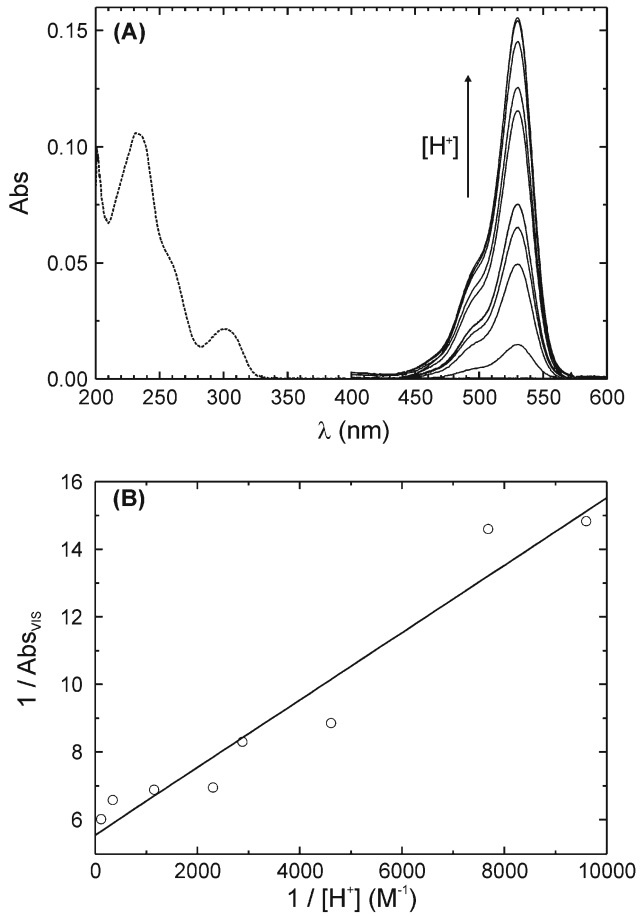

Fig. 1 (A) Absorption spectra of the SF form of compound **5** in pure ethanol (dashed line), and after the equilibrium was reached using increasing amounts of acid: from bottom to top, the analytical concentrations of acid are: 1.0×10^{-4} M, 1.3×10^{-4} M, 2.1×10^{-4} M, 3.5×10^{-4} M, 4.3×10^{-4} M, 8.7×10^{-4} M, 2.9×10^{-3} M, 8.7×10^{-3} M. (B) Plot of the absorption data in A according to eqn (1).

Table 1 Equilibrium constants for the ring opening of compounds **1–6** at room temperature, absorption coefficients of the SF and OFH^+ isomers, and emission quantum yields of the OFH^+ isomers

			ε (10^4 M^{-1} cm^{-1})[b]		
Compound	K_{eq} (M^{-1})	logK_{eq} (M^{-1})[a]	SF (313 nm)	OFH^+ (max)	ϕ_{fluo}[c]
1	2.7×10^3	3.4	1.0	4.3	0.50
2	1.9×10^3	3.3	1.3	4.9	0.45
3	8.3×10^2	2.9	0.9	6.3	0.51
4	5.0×10^2	2.7	1.0	n.d.[d]	0.40
5	5.6×10^3	3.8	0.7	6.8	0.94
6	4.2×10^2	2.6	0.5	2.8	0.87

[a] Standard deviation is ±0.3 units. [b] Standard deviation is ±20%. [c] Standard deviation is ±0.1 units. [d] Not detected

times were obtained by single exponential fits (see below). First, we measured the dark equilibration kinetics; after a pH jump was induced in pure ethanol by addition of TFA (the first order rate constant of this process is named k_{H^+}). Second, the photoinduced isomerization at a fixed pH value after attaining dark equilibration was followed under UV irradiation (first order rate

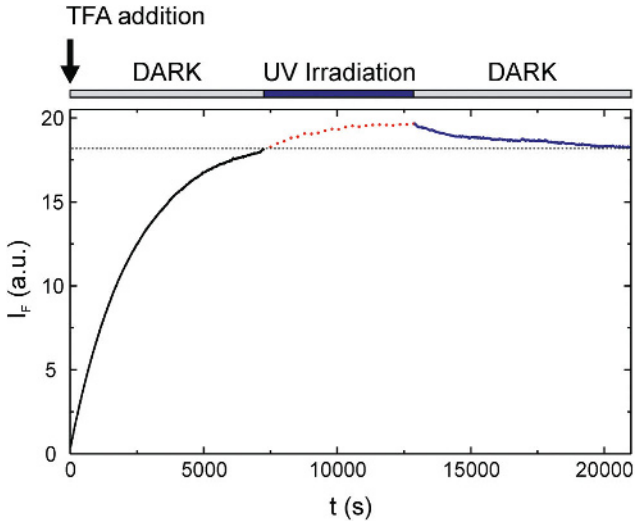

Fig. 2 A full kinetic experiment for compound **2** after TFA is added at $t = 0$ to a final concentration of 9.83×10^{-4} M. In this experiment, the three processes are monitored by fluorescence emission of OFH^+ at 580 nm (λ_{exc} = 520 nm). UV irradiation was performed at 315 nm for the period indicated. The horizontal dotted line indicates the emission intensity in the dark equilibrium state.

constant k_{PH}). Third, the dark recovery from the photostationary state to the dark equilibrium state was monitored (first order rate constant k_{Th}). An example of a full kinetic cycle for compound **2** at a 9.83×10^{-4} M TFA is shown in Fig. 2. It is expected that $k_{H^+} = k_{Th}$ in all cases, as both are measuring the dark relaxation only from different initial conditions, namely excess of SF with respect to the equilibrium state for k_{H^+}, and excess of OFH^+ for k_{Th} (see discussion).

All kinetic traces rendered good fits to single exponential functions within experimental error (some examples of the kinetic fits are given in Fig. S1–S3 of the ESI‡). The kinetic constant for the three processes studied, k_{H^+}, k_{PH} and k_{Th}, showed a linear relation with proton concentration, as presented in Fig. 3 for compounds **2**, **3**, and **5**, with a near zero intercept. The slopes of the plots like those of Fig. 3 for all the compounds are summarized in the ESI‡ (Section C).

Discussion

The transformation from SF to OFH^+ involves a bond dissociation (the C9–N bond) and a protonation step. Both are considered to be reversible kinetically. In the dark, the protonation of SF can be considered to be a much faster step than the ring opening and to be practically at equilibrium during the bond scission event.

In the photochemical process, the C9–N bond of SF is most probably broken and the open form OF is afterwards protonated to yield $OF–H^+$, the final stable isomer. It is unlikely that the excited state of SF can be protonated due to its short lifetime (as no fluorescence from SF is detected, the lifetime of its first excited singlet state is assumed to be less than 0.1 ns determined by non-radiative relaxation to the ground state). As both species are in equilibrium in the dark, both SF and $SF–H^+$ absorb at the UV irradiation wavelength and yield OF or $OF–H^+$, respectively,

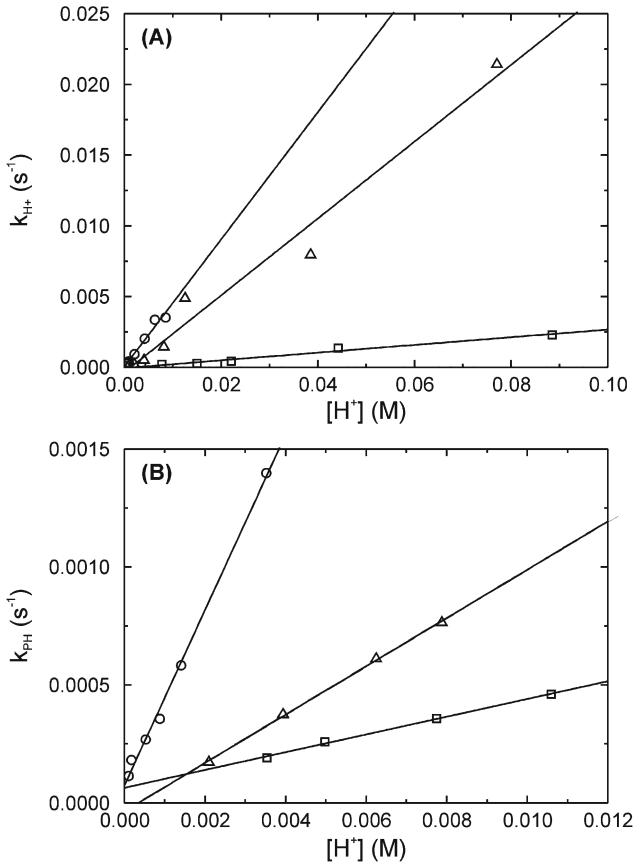

Fig. 3 k_{H^+} (A) and k_{PH} (B) for compounds **2** (circles), **3** (triangles), and **5** (squares) as a function of proton concentration.

with quantum yields that can be dependent on the protonation state.

In view of these considerations, we propose the mechanism of Scheme 4. This mechanism is similar to the acidochromic ring opening of spiropyrans, also involving protonation and a bond scission step.[24]

To solve this mechanism for the build up rate of OFH^+, we will first consider only the thermal pathway, and then add afterwards the photochemical steps to obtain the characteristic times under irradiation. The thermal pathway involves a protonation–deprotonation step and a bond scission–formation. They are characterized by rate constants k_1–k_4. Of these, three have the first order rate constants k_2, k_3, and k_4, while one has a pseudo first order rate constant $k_1 \cdot [H^+]$. This simplified version of Scheme 4 is depicted in Scheme 5.

Taking into account that the build up of OFH^+ is single exponential at the observed time window, one of the two relaxation times of Scheme 5 should be fast in the seconds time window. Assuming that the protonation step is at equilibrium, the build up of OFH^+ should follow a first order rate law. Considering that the protonation step is much faster than the ring opening step, *i.e.* k_1 $[H^+]$; $k_2 \gg k_3$; k_4, the build up rate for OFH^+ is (see ESI‡ for the derivation):

$$\left(\frac{d[OFH^+]}{dt}\right)_{Th} = \left(\frac{k_3 \cdot k_1 \cdot [H^+]}{k_2} + k_4\right) \cdot [SF] - k_4 \cdot C_0 \qquad (2)$$

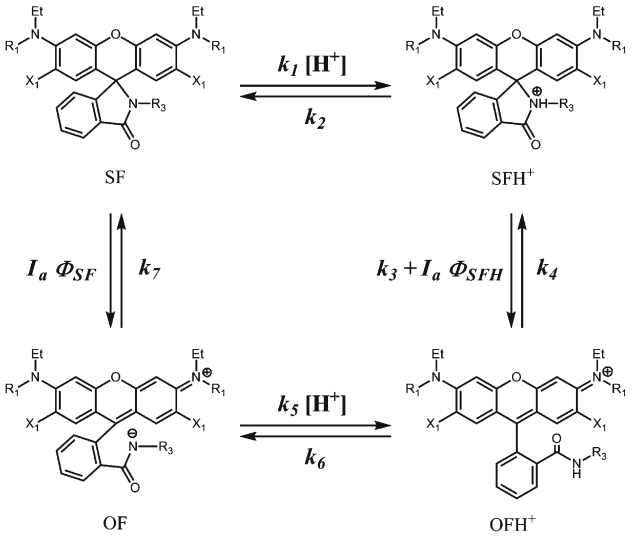

Scheme 4 Proposed mechanism for the proton and photoinduced isomerization of spirorhodamines.

Scheme 5 Reaction mechanism for the thermal pathway.

where C_0 is the total concentration, of SF and OF species. Eqn (2) can be integrated to give a first order build up rate with a characteristic time, τ, that depends linearly on $[H^+]$, according to the following equations (see ESI‡ for the derivation).

$$[OFH^+]_{Th}(t) = C_0 \cdot \left\{1 - \tau_{Th} \cdot \left(\frac{k_3 \cdot k_1 \cdot [H^+]}{k_2} \exp(-t/\tau_{Th}) + k_4\right)\right\} \qquad (3a)$$

$$\frac{1}{\tau_{Th}} = k_{Th} = \frac{k_3 \cdot k_1 \cdot [H^+]}{k_2} + k_4 \qquad (3b)$$

Under irradiation in the UV, the reaction shown in Scheme 4 accounts for the rate observed. Because all kinetic experiments were carried out under low absorbance conditions at the irradiation wavelength (A (315 nm, 1 cm) <0.1), the light absorption rate is proportional to the concentration of the absorbing species (SF or SFH^+), and, consequently, the photochemical rate follows a first order process. In line with the assumption made for the thermal reaction, we can consider that the protonation step of OF is faster than the ring closure to SF. This means that k_5 $[H^+] \gg k_7$. Under these two approaches, the rate of build up of OFH^+ under continuous irradiation takes the form:

$$\left(\frac{d[OFH^+]}{dt}\right)_{PH} = \left(\frac{(k_3 + k_{PH,SFH+}) \cdot k_1 \cdot [H^+]}{k_2} + k_{PH,SF} + k_4\right) \cdot [SF] - k_4 \cdot C_0 \qquad (4)$$

$k_{PH,SFH}$ and $k_{PH,SF}$ are the inverse of the purely photochemical relaxation times, and have the following expressions:

$$k_{PH,SF} = I_0 \cdot \ln 10 \cdot l \cdot \varepsilon_{SF}^{UV} \cdot \Phi_{SF} \quad (5a)$$

$$k_{PH,SFH+} = I_0 \cdot \ln 10 \cdot l \cdot \varepsilon_{SFH}^{UV} \cdot \Phi_{SFH^+} \quad (5b)$$

where I_0 is the incident photon flux rate, and Φ_{SF}, Φ_{SFH^+} are the quantum yields for ring opening for SF and SFH^+, respectively. Eqn (4) is very similar to eqn (2). It also predicts a first order build up of OFH^+, with a characteristic time of:

$$\frac{1}{\tau_{PH}} = k_{PH} = \frac{(k_3 + k_{PH,SFH+}) \cdot k_1 \cdot [H^+]}{k_2} + k_{PH,SF} + k_4 \quad (6)$$

The proton concentration dependence in eqn (6) is also linear, with a slope and intercept that are modified by the addition of the photochemical *pseudo* rate constants.

In addition, the relation between the equilibrium constant and the rate constants for each step is:

$$K_{eq} = \frac{k_1 \cdot k_3}{k_2 \cdot k_4} \quad (7)$$

The mechanism predicts a linear dependence of k_{H^+}, and k_{Th}, the inverse of the relaxation time of the thermal process, with $[H^+]$, with a $k_{slope,H^+} = k_{slope,Th} = (k_1 \cdot k_3)/k_2 = k_4 \cdot K_{eq}$, and an intercept $k_{0,H^+} = k_{0,Th} = (k_{PH,SF} + k_4)$. Therefore, in both cases, a linear fit of the inverse of the measured characteristic times as a function of the proton concentration yields k_4 as the intercept and $(k_4 \cdot K_{eq})$ as the slope. The results show that k_4 is negligible within the precision of our measurements, and confirms the linear dependence of the measured constants with proton concentration.

Under continuous irradiation, again there is a linear dependence of the inverse of the relaxation time (k_{PH}) with $[H^+]$ with a slope $k_{slope,PH} = (k_3 + k_{PH,SFH^+}) \cdot k_1/k_2$, which should be larger than the slope of the thermal processes. For the intercept, $k_{0,PH} = k_4 + k_{PH,SF}$, an increase is predicted as well for the photochemical relaxation step. However, an analysis of the results of Fig. 2 and 3 shows that the differences introduced by the photoinduced component of the initiation process are too small and fall within experimental uncertainty of the kinetic determinations. Thus, we conclude that $k_{slope,PH} = k_{slope,Th} = (k_1 \cdot k_3)/k_2$.

Fig. 4 shows the correlation between the three slopes of k_{H^+}, k_{PH}, and k_{Th} and log K_{eq} for each compound. Within a reasonable experimental uncertainty of ±0.3 units in $k_{slope,PH}$ and $k_{slope,Th}$ all values are equal for each compound.

The similarity between the slopes can be well understood if we analyze eqn (3b) and (6) and the results are depicted in Fig. 2. The latter shows that the difference in concentration between the dark equilibrium state and the photostationary state is within 20% for the more abundant species. In addition, with the conclusion that all three experimental slopes are equal we can relate the kinetic constants with K_{eq}: through eqn (8).

$$k_{slope,PH} \approx k_{slope,Th} = k_{slope} = \frac{(k_1 \cdot k_3)'}{k_2} = k_4 \cdot K_{eq} \quad (8)$$

The latter explains the linear correlation between log(k_{slope}) and log(K_{eq}) with a slope of 1.4 ± 0.3. Furthermore, this linear

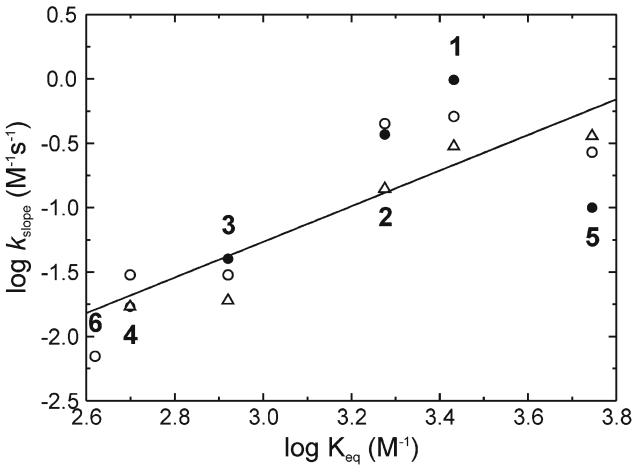

Fig. 4 Correlation between the first order kinetic rate constants k_{H^+} (open circles), k_{PH} (filled circles), and k_{Th} (triangles) and the equilibrium constant for the proton induced ring opening, K_{eq} (see Scheme 3). A linear fit renders a slope of 1.4 ± 0.3 and an intercept of −6 ± 1.

relation means that k_4 is approximately equal for all compounds. The value, given by the intercept of the plot of Fig. 4, has a very high uncertainty: log(k_4) [s^{-1}] = −6.0 ± 1.0.

We will now discuss the influence of molecular structure on the position of the equilibrium for the photochromic transformation reaction. The predictability of the tendency in K_{eq} becomes more relevant in view of its correlation with the kinetics of the transformation.

The complete transformation of the spirorhodamine involves two successive steps. One of the steps is a rearrangement involving a ring aperture whose equilibrium position is a compromise between the strength of the C9–N spiro bond, the nucleophilicity of the amide group and the electron density in the C9 in the open form. The presence of an aromatic substituent in the amide group (compounds **1** and **2**) lowers the nucleophilicity, whereas the presence of two alkyl groups in R_1 (compounds **1**–**4**) increases the electron density in the C9 in the OF, disfavoring the nucleophilic attack by the amide group. These factors contribute to shift the position of the equilibrium to the SF isomer in compounds **1** and **2**, and to OF^- in compounds **5** and **6**; while compounds **3** and **4** are expected to display an intermediate behavior.

The other step is an equilibrium which depends on the acidity of the protonated lactam. In this case, the aromatic group renders the N more acidic, hindering protonation and shifting this equilibrium towards the deprotonated form. Neither the substituents in R_1 nor X_1 are expected to influence the position of the equilibrium of this step.

The previous discussion shows compensating effects of the structure in the value of K_{eq} for compounds **5** and **6** and leads us to expect a higher value of K_{eq} for compounds **3** and **4** compared to **1** and **2**. The actual values of K_{eq} (see Table 1) are at the extreme for **5** (the highest) and for **6** (the lowest), whereas **3** and **4** have lower values of K_{eq} than **1** and **2**.

The highest and the lowest equilibrium constants differ in 0.8 logarithmic units. This difference is equivalent to 4.6 kJ mol^{-1} at room temperature (300 K), too low to be explained by coarse substituent effects. Nevertheless, the previous discussion clearly

shows compensating effects that render prediction difficult, and the importance of other effects neglected in the discussion, such as steric hindrance or the strength of the spiro carbon –N bond in the SF form.

Conclusions

As a conclusion, we find that the constants for the three observed processes are similar under the experimental accuracy and there is a good correlation between the kinetic constant and the equilibrium constant (acidic constant) for the series of six studied compounds. Nevertheless, we see a clear difference between the amounts of the protonated open form in a thermal equilibrium and in the photostationary state (see for example Fig. 2).

For compounds **1–6** at a proton concentration in the range 10^{-3} to 10^{-4} M, equal amounts of OFH^+ and SF are present at equilibrium. Therefore, they can be used as fluorescent pH indicators in such ranges.[25,26] At a ten-fold higher proton concentration, complete conversion to the OFH^+ can be attained, while at a H^+ concentration in the range 10^{-4} to 10^{-5} M (or higher) the system is predominantly in the SF colorless form. This later situation is the most desirable for the use of the dye in super-resolution microscopy.

Acknowledgements

MLB and PFA are research staff from CONICET (Miembros de la carrera del investigador científico del Consejo Nacional de Investigaciones Científicas y Técnicas, Argentina). This work was performed under support from UBA (Grant Numbers X006, and 20020090300147) and ANPCyT, Argentina (PICT 33973, PICT PRH 2008 N° 0173), and the Max Planck Society, Germany (Partner Group Grant). We thank Dr Vladimir Belov (Department of NanoBiophotonics, Max-Planck-Institut für Biophysikalische Chemie, Göttingen, Germany) for providing compounds **1** and **2**.

References

1 *Photochromism. Molecules and Systems*, ed. H. Dürr and H. Bouas-Laurent, Elsevier, Amsterdam, 1990.
2 *Organic Photochromic and Thermochromic Compounds*, ed. J. C. Crano and R. J. Guglielmetti, Plenum Press, New York, 1999.
3 Photochromism. Molecules and switches. Thematic issue. Chem. Rev., 100 Issue 5, 2000.
4 G. Favaro and M. Irie, ed., Special issue on photochromism, *J. Photochem. Photobiol., C: Photochem. Rev.*, 2011, **12**, 71–236.
5 A. Natansohn and P. Rochon, Photoinduced motions in azo-containing polymers, *Chem. Rev.*, 2002, **102**, 4139–4175.
6 K. Ichimura, Photoalignment of liquid-crystal systems, *Chem. Rev.*, 2000, **100**, 1847–1874.
7 M. Yamada, M. Kondo, J. Mamiya, Y. Yu, M. Kinoshita, C. J. Barrett and T. Ikeda, Photomobile polymer materials: towards light driven plastic motors, *Angew. Chem., Int. Ed.*, 2008, **47**, 4986–4988.
8 D. A. Davis, A. Hamilton, J. Yang, L. D. Cremar, D. Van Gough, S. L. Potisek, M. T. Ong, P. V. Braun, T. J. Martínez, S. R. White, J. S. Moore and N. R. Sottos, Force-induced activation of covalent bonds in mechanoresponsive polymeric materials, *Nature*, 2009, **459**, 68–72.
9 S. W. Hell, Toward fluorescence nanoscopy, *Nat. Biotechnol.*, 2003, **21**, 1347–1355.
10 S. W. Hell, Far-field optical nanoscopy, *Science*, 2007, **316**, 1153–1158.
11 S. W. Hell, Microscopy and its focal switch, *Nat. Methods*, 2009, **6**, 24–32.
12 K.-H. Knauer and R. Gleiter, Photochromism of rhodamine derivatives, *Angew. Chem., Int. Ed. Engl.*, 1977, **16**, 113.
13 J. Fölling, V. Belov, R. Kunetsky, R. Medda, A. Schönle, A. Egner, C. Eggeling, M. Bossi and S. W. Hell, Photochromic rhodamines provide nanoscopy with optical sectioning, *Angew. Chem., Int. Ed.*, 2007, **46**, 6266–6270.
14 J. Fölling, V. Belov, D. Riedel, A. Schönle, A. Egner, C. Eggeling, M. Bossi and S. W. Hell, Fluorescence nanoscopy with optical sectioning by two-photon induced molecular switching using continuous-wave lasers, *ChemPhysChem*, 2008, **9**, 321–326.
15 T. Karstens and K. Kobs, Rhodamine B and rhodamine 101 as reference substances for fluorescence quantum yield measurements, *J. Phys. Chem.*, 1980, **84**, 1871–1872.
16 D. Magde, G. E. Rojas and P. G. Seybold, Solvent dependence of the fluorescence lifetimes of xanthene dyes, *Photochem. Photobiol.*, 1999, **70**, 737–744.
17 H. Willwohl, J. Wolfrum and R. Gleiter, Kinetics and mechanism of the photochromism of *N*-phenyl-rhodaminelactame, *Laser Chem.*, 1989, **10**, 63–72.
18 M. Bossi, J. Fölling, V. N. Belov, V. P. Boyarskiy, R. Medda, A. Egner, C. Eggeling, A. Schönle and S. W. Hell, Multicolor far-field fluorescence nanoscopy through isolated detection of distinct molecular species, *Nano Lett.*, 2008, **8**, 2463–2468.
19 I. Testa, A. Schönle, C. v. Middendorff, C. Geisler, R. Medda, C. A. Wurm, A. C. Stiel, S. Jakobs, M. Bossi, C. Eggeling, S. W. Hell and A. Egner, Nanoscale separation of molecular species based on their rotational mobility, *Opt. Express*, 2008, **16**, 21093–21104.
20 V. N. Belov, M. L. Bossi, J. Fölling, V. P. Boyarskiy and S. W. Hell, Rhodamine spiroamides for multicolor single-molecule switching fluorescent nanoscopy, *Chem.–Eur. J.*, 2009, **15**, 10762–10776.
21 M. Adamczyk and J. Grote, Efficient synthesis of rhodamine conjugates through the 2′-position, *Bioorg. Med. Chem. Lett.*, 2000, **10**, 1539–1541.
22 M. Adamczyk and J. Grote, Synthesis of novel spirolactams by reaction of fluorescein methyl ester with amines, *Tetrahedron Lett.*, 2000, **41**, 807–809.
23 M. Adamczyk and J. Grote, Synthesis of probes with broad pH range fluorescence, *Bioorg. Med. Chem. Lett.*, 2003, **13**, 2327–2330.
24 J. T. C. Wojtyk, A. Wasey, N.-N. Xiao, P. M. Kazmaier, S. Hoz, C. Yu, R. P. Lemieux and E. Buncel, Elucidating the mechanisms of acidochromic spiropyran-merocyanine interconversion, *J. Phys. Chem. A*, 2007, **111**, 2511–2516.
25 Q. A. Best, R. Xu, M. E. McCarroll, L. Wang and D. J. Dyer, Design and investigation of a series of rhodamine-based fluorescent probes for optical measurements of pH, *Org. Lett.*, 2010, **12**, 3219–3221.
26 X. Chen, T. Pradhan, F. Wang, J. S. Kim and J. Yoon, Fluorescent chemosensors based on spiroring-opening of xanthenes and related derivatives, *Chem. Rev.*, 2012, **112**(3), 1910–1956.

